Published in final edited form as:
Cancer Res. 2005 September 1; 65(17): 7824–7831.

Effect of platelet derived growth factor receptor-β inhibition with STI571 on radioimmunotherapy

Janina Baranowska-Kortylewicz*[1], **Michio Abe**[1], **Kristian Pietras**[3], **Zbigniew P. Kortylewicz**[1], **Takashi Kurizaki**[2], **Jessica Nearman**[1], **Janna Paulsson**[4], **R. Lee Mosley**[5], **Charles A. Enke**[1], and **Arne Östman**[4]

1*Department of Radiation Oncology, University of Nebraska Medical Center, Omaha, Nebraska, USA*

2*Department of Surgery II, National Hospital Organization, Kumamoto University Medical School, Kumamoto, Japan*

3*Ludwig Institute for Cancer Research, Karolinska Institute, Stockholm, Sweden*

4*Department of Pathology-Oncology, Karolinska Institute, Stockholm, Sweden*

5*Department of Pathology and Microbiology, University of Nebraska Medical Center, Omaha, Nebraska, USA*

Abstract

While radioimmunotherapy of hematological malignancies has evolved into a viable treatment option, the responses of solid tumors to RADIOIMMUNOTHERAPY are discouraging. The likely cause of this problem is the interstitial hypertension inherent to all solid tumors.

Remarkable improvements in tumor responses to radioimmunotherapy were discovered after the inclusion of STI571 in the therapy regimen. A combination of the tumor stroma-reactive STI571, a potent PDGFr-β antagonist, and the tumor-seeking radiolabeled antibody B72.3 yielded long-lasting growth arrest of the human colorectal adenocarcinoma LS174T grown as subcutaneous xenografts in athymic mice. The interaction of STI571 with the stromal PDGFr-β reduced tumor interstitial fluid pressure (P_{IF}) by >50% and in so doing improved the uptake of B72.3. The attenuation of P_{IF} also had a positive effect on the homogeneity of antibody distribution. These effects were dose-dependent and under optimized dosing conditions allowed for a 2.45× increase in the tumor uptake of B72.3 as determined in the biodistribution studies. SPECT imaging studies substantiated these results and indicated that the homogeneity of the radioisotope distribution was also much improved when compared to the control mice. The increased uptake of radioimmunotherapy into the tumor resulted in >400% increase in the tumor absorbed radiation doses in STI571+RIT-treated mice compared to PBS+RIT-treated mice.

The improved antibody uptake in response to the attenuation of tumor P_{IF} was identified as the primary reason for the growth arrest of the STI571+RIT-treated tumors. Two related causes were also identified: (1) the improved homogeneity of MAb distribution in tumor; and (2) the increased tumor radiosensitivity resulting from the improved tumor oxygenation.

Keywords

radioimmunotherapy; STI571; adenocarcinoma; interstitial fluid pressure; PDGF receptor β

[1]Financial support for these studies was provided by the NIH grant R01CA95267-01 (JBK), LB506 grant funded by the Nebraska Department of Health (JBK), and a postdoctoral fellowship from the Swedish Cancer Society (KP).
[2]Reprint requests should be sent to Janina Baranowska-Kortylewicz, University of Nebraska Medical Center, Department of Radiation Oncology, 986850 Nebraska Medical Center, Omaha, NE 68198-6850, e-mailjbaranow@unmc.edu.

Introduction

Radioimmunotherapy (RIT), i.e., using monoclonal antibodies (MAb) coupled to radioactive isotopes as tumoricidal agents, has gained a prominent place in the treatment of lymphoma. Radioimmunotherapy allows for a selective recognition and killing of malignant cells while sparing normal tissues. Impressive responses to radioimmunotherapy have been observed in non-Hodgkin's lymphomas, even in a chemotherapy-relapsed and refractory disease (1–3). Two agents (^{90}Y-ibritumomab tiuxetan and ^{131}I-tositumomab) have already been approved by the US Food and Drug Administration. High response rates and durable remissions in various subtypes of B-cell non-Hodgkin's lymphomas confirmed a single-agent efficacy of radioimmunotherapy in this disease (2,3) and prompted several combination therapy clinical trials to further improve the outcome.

By contrast, solid tumors have proven thus far resistant to MAb-based radiotherapies (4–6). Efficient delivery of radioimmunotherapy to solid tumors encounters numerous physical barriers. Compromised tumor vasculature, slow diffusion and convection rates of large MAb molecules through the interstitial spaces, and high intratumoral pressures hinder MAb influx into tumors. As a result, MAb do not penetrate tumors uniformly. Instead, they tend to accumulate in the periphery of the tumor and in the perivascular zones (7–10). In order to reach all clonogenic tumor cells, MAb must cross the tumor endothelium and its underlying basement membrane, and filter through the tumor stroma and parenchyma. Notwithstanding the fact that tumor vessels are abnormally leaky to macromolecules, the extravasation of MAb into the tumor mass is inefficient (9–11). In clinical studies, tumor deposits at levels as low as 0.001–0.01% of the injected dose of radiolabeled antibody per gram of tumor are commonplace. Estimates of absorbed radiation doses range from 100 to 3000 cGy and indicate that the majority of MAb fails to extravasate at the tumor site (see for example 5,12, and 13). To date, advances in radioimmunotherapy to treat solid tumors are lackluster. Various efforts to improve the MAb accretion in solid tumors and consequently to improve the efficacy of radioimmunotherapy have been instigated (4,11,14–18).

High interstitial fluid pressure (P_{IF}) is a property displayed by many solid tumors. P_{IF} creates a formidable physiological barrier to tumor uptake of drugs from circulation and is largely responsible for the inefficient uptake of radioimmunotherapy (10,19–21). Several recent studies have identified platelet-derived growth factor (PDGF) as a critical regulator of P_{IF} in normal loose connective tissue and solid tumors (22–26). PDGF regulation of P_{IF} in loose connective tissue was first demonstrated by Rodt *et al*. in a rat model of anaphylaxis-induced attenuation of P_{IF}. Local injections of PDGF-BB normalized P_{IF}, implying that stromal cells actively control P_{IF} (25). In a similar model, the activation of phosphatidylinositol-3′-kinase through the PDGF-BB interaction with PDGFr-β was found to be critical for the control of P_{IF} in the loose connective tissue (26).

A novel mechanism for therapeutic synergy between PDGFr-β antagonists and chemotherapeutic agents has been proposed by Pietras *et al*. (22), based on their observation that STI571, a potent PDGFr-β inhibitor significantly reduces tumor P_{IF} and augments accretion of Taxol in subcutaneous (SQ) tumors in mice. Subsequent studies in tumor models having PDGFr-β expression restricted to stromal cells confirmed that the reduction in tumor P_{IF} after treatment with PDGF inhibitors results in improvements in the tumor uptake of chemotherapeutic drugs (23,24). The attenuation of tumor P_{IF} suggests that STI571 has the capacity to engage PDGFr-β in cells of tumor stroma. In all probability, the STI571-induced decrease in P_{IF} improves the capillary-to-interstitium transport rate in subcutaneous tumors by antagonizing PDGFr-β.

For this reason, a combination STI571-RIT emerged as a regimen that may well allow accumulation of therapeutically sufficient radiation doses in solid tumors. STI571 (Gleevec®, imatinib mesylate) is a tyrosine kinase inhibitor that blocks tyrosine kinases of abl, c-kit and PDGF receptors. STI571 has been approved by the FDA in 2001 for the treatment of chronic myelogenous leukemia (CML) and gastrointestinal stromal tumors, where it acts by inhibition of bcr-abl and mutated c-kit, respectively (27). It is noteworthy that edema and fluid retention are the most common side effects after the prolonged STI571 treatment in CML patients. Although the mechanism for these problems remains to be fully characterized, one obvious process appears to be via the inhibition of PDGFr-β (28,29).

The efficacy of the STI571-RIT regimen was evaluated in a human colorectal adenocarcinoma LS174T xenografted in athymic mice. LS174T tumors grown as SQ xenografts express mucin-like tumor-associated glycoprotein-72 (TAG-72), to which MAb B72.3 was developed (30, 31). The treatment of LS174T-bearing mice with ^{131}I-B72.3 produces some tumor growth arrest at doses 0.3 mCi or greater (>10 MBq) (32). At these doses, severe radiotoxicity was readily evident with a lethal bone marrow aplasia in >20% of mice. Although ^{111}In-labeled B72.3 (Oncoscint, satumomab pendetide) was the first labeled MAb to be approved by the FDA for tumor imaging, neither B72.3 nor its higher affinity, second generation analog MAb CC49 labeled with either ^{131}I or ^{90}Y, have shown any therapeutic efficacy in clinical trials (5,33).

Materials and Methods

Animal and Tumor Models.

Four- to six-weeks old athymic female mice (NCr-nu/nu), average weight 18 g, were purchased from the National Cancer Institute Animal Program. Fox Chase SCID mice of a similar age and weight were purchased from M&B (Ry, Denmark). Mice were housed in a fully accredited by AAALAC Animal Facilities. Mice were acclimated for 5–7 days after arrival before any experiments. All procedures described here were approved by the local IACUC. Mice had a free access to food and water and were kept on a 12-hour light cycle. Potassium iodide-supplemented water was provided for 3 days before and 4 days after any treatment with radioiodinated antibodies. Subcutaneous tumors were produced in these mice approximately 10 days after the SQ injection of 5×10^6 LS174T human colorectal adenocarcinoma cells in 0.2 mL minimum essential medium (MEM, Invitrogen, Carlsbad, California). The cells were obtained from sub-confluent monolayers grown in the MEM supplemented with 10% fetal bovine serum.

Reagents.

Mouse monoclonal antibody B72.3 was produced by the UNMC Monoclonal Antibody Facility. It was purified from mice ascites by protein-G-affinity chromatography. B72.3 recognizes a high molecular weight glycoprotein complex designated as a tumor associated glycoprotein-72 (TAG-72) and shows reactivity with over 85% of adenocarcinomas with minimal reactivity to normal tissues (31). Goat anti-PDGF β-receptor antibody P-20 (Santa Cruz Biotechnology, Santa Cruz, CA), monoclonal antiphosphotyrosine antibody PY20 (Transduction Laboratories, Lexington, KY) were used as recommended by the suppliers. STI571 (Gleevec®, imatinib mesylate) was generously provided by Novartis Pharma AG. The stannylated precursor of the nitroimidazole-based radioiodinated hypoxia tracer 1-[ethyl-(3′-[^{125}I]iodobenzamide)]-2-nitroimidazole was prepared on site. The radioiodination was also performed on site. Sodium iodide-125 and iodide-131 were purchased from PerkinElmer Life and Analytical Sciences, Inc. (Boston, MA). Iodine-125 radionuclide had a specific activity of ~17 Ci (629 GBq)/mg and was provided in a 10^{-5} M NaOH (pH 8–11) (without reductants) at a concentration of 100mCi/mL (3.7 GBq/mL). Iodine-131 radionuclide had a specific activity

of >5 Ci (>185 GBq)/mg and was provided in 0.1 M NaOH (pH 12–14). Antibodies were radioiodinated using the Iodogen method (34) as follows. Iodine-125 radiolabeling was done in a glass test tube coated with 0.05 mg of Iodogen. One hundred μL of 1 mg/mL solution of B72.3 in phosphate buffered saline, pH 7.2 (0.01 M phosphate buffer, 0.0027 M potassium chloride and 0.137 M sodium chloride, pH 7.2 at 25 °C) and 0.1 mL of iodine-125 (1.0 mCi; 37 MBq) was transferred into the Iodogen-coated tube. The mixture was incubated at room temperature for 10–20 min. The reaction progress was measured using instant thin layer chromatography with a methanol/water (1:4; v/v) as the elution system. ^{125}I-B72.3 was purified on an Econo-Pac® 10DG gel filtration column (Bio-Rad Laboratories, Hercules, CA) eluted with PBS. For therapy studies, B72.3 was labeled with iodine-131 as follows: into a glass test tube coated with 0.1 mg of Iodogen was added 0.1 mL of 10 mg/mL B72.3 in PBS, pH 7.2 and 0.01 mL of iodine-131 (10 mCi; 370 MBq). The mixture was incubated at room temperature for 20 min. The reaction progress was measured using instant thin layer chromatography with a methanol/water (1:4; v/v) as the elution system. ^{131}I-B72.3 was also purified on a 10DG gel filtration column eluted with PBS. Before administration radiolabeled antibodies were diluted with PBS containing 0.1% mouse serum to yield the injection dose volume of 0.2 mL per mouse.

In vitro cell growth assay.

LS174T cells were seeded in 96-well plates at a density of 3,000 cells per well in either full growth medium (Eagle Minimum essential medium with 2 mM L-glutamine and Earle's BSS adjusted to contain 1.5 g/L sodium bicarbonate, 0.1 mM non-essential amino acids, and 1.0 mM sodium pyruvate, supplemented with 10% fetal bovine serum) or serum-depleted growth medium containing 0.1% bovine albumin. After 24 h of growth, the culture medium was replaced with fresh medium containing 0, 0.1, 1.0 or 5.0 μM STI571 and the cells were allowed to grow for 24 or 48 h, n=6 wells per concentration and time point. Subsequently, a colorimetric assay (CellTiter 96® AQueous One Solution Cell Proliferation Assay, Promega, Madison, WI) was used to measure the metabolic activity of cells. The fractional growth of untreated control cells was set to 100%.

In vitro radiosensitization assay.

The *in vitro* radiosensitization assay was performed as described above for the *in vitro* cell growth assay with the addition of irradiation of STI571-treated cells at two radiation doses: 1 Gy or 6 Gy at 1.9 Gy/min in the Mark I 68A research irradiator (6,000 Ci Cesium-137 source, J.L. Shepherd and Associates, San Fernando, CA). Subsequently, cells were allowed to grow for 48 h before the cell proliferation was determined using the colorimetric kit. The proliferating fraction of cells irradiated in the absence of any additional treatment was set to 1 or 100%.

Immunoblotting.

LS174T cells and porcine aortic endothelial cells - positive control (35) expressing both PDGF receptor-α and -β (American Type Culture Collection, Manassas, VA) were seeded in 60-mm dishes (1.5×10^6 cells/dish) and starved overnight in cell culture medium containing antibiotics and 0.1% BSA. Next, cells were stimulated or not with 100 ng/mL PDGF-BB for 7 min at 37° C. All subsequent treatments were as described previously (22–24,36,37).

Immunohistochemistry.

The expression of PDGfr-β was determined in de-paraffinized, formalin-fixed sections from untreated LS174T xenografts as described previously for KAT-4 (23).

Effect of STI571 on in vivo phosphorylation of PDGFr-β.

Two methods were employed to determine the levels of PDGFr-β phosphorylation in the STI571-treated LS174T tumors. The first method used was as described by Pietras et al. (23) without any modifications. Quantification of blotted protein band intensities was performed on a CCD-camera (Fuji Film). The intensity of the phospho-tyrosine signal was divided by the intensity of the receptor signal to yield relative phospho-tyrosine values. The average relative phospho-tyrosine value of PBS-treated tumors was set to 1. The second method used the PathScan® phospho-PDGFr-β sandwich ELISA kit (Cell Signaling Technology, Inc., Beverly, MA). After the protein content in tumor lysates was determined, aliquots were prepared containing 0.6 mg total protein and the volume of each sample was adjusted to 0.1 mL with PBS. From this point on, the protocol provided with the ELISA kit was followed without any modifications.

Measurement of the tumor P_{IF}.

Tumor P_{IF} was measured by the wick-in-needle technique, as described previously (22,23). STI571 was administered by gavage BID for a total dose of 100 $mg\times kg^{-1}\times day^{-1}$ in 200 μL of PBS (n=5) for four consecutive days before the measurement of the tumor P_{IF}. Control mice were given PBS (n=6). The last administration of STI571 preceded the measurement of the tumor P_{IF} by 1–2 h.

Biodistribution.

Mice were treated with either PBS or STI571 for ten consecutive days as indicated in Table 1 for a total dose of 100 $mg\times kg^{-1}\times day^{-1}$. Radiotracer ^{125}I-B72.3 (10 μCi/mouse) was injected IV via a tail vein (PBS control group n=8; STI571 group n=11). All mice were killed 120 h after ^{125}I-B72.3 administration, tumors were removed, and the amount of radioactivity in tumor, blood and selected tissues was measured. The tissue and tumor uptake are expressed as percent injected dose per gram tumor.

Radioimmunotherapy.

Mice were randomized into four groups: (1) no treatment (n = 10); (2) ^{131}I-B72.3 only (n = 10); (3) STI571 only (n = 12); and (4) ^{131}I-B72.3 plus STI571 (n = 12). Body weight and tumor sizes were measured three times a week, and tumor volumes calculated according to the following formula: $volume=\pi/6\times longer\ diameter\times (shorter\ diameter)^2$. STI571 was administered as indicated in Table 1 and ^{131}I-B72.3 (0.25 mCi) was injected IV via a tail vein in 0.2 mL PBS on day 0, 1–2 h after PO dose of STI571. Before termination of the experiment, all mice were injected with 50 μCi ^{125}IUdR to enable measurement of the tumor proliferative rate. Excised tumors were lysed and the amount of ^{125}IUdR bound to DNA was determined using the DNA Extractor WB Kit - Sodium Iodide method (Wako Chemicals USA, Inc, Richmond, VA).

Imaging studies.

Four mice with size-matched tumors (1.9 g – 2.1 g) were selected from groups treated with either STI571 (n = 2) or PBS (n = 2; control), as shown in Table 1. ^{125}I-B72.3 was injected intravenously (IV) and the imaging commenced 24 h after the administration of the radioactive tracer. Images were acquired using a dedicated Animal SPECT Imaging System (Gamma Medica Instruments, Northridge, CA)[3]. The images were reconstructed using LumaGEM version 5.107 software with the Butterworth bandpass post-reconstruction filtering. To obtain quantitative evaluation of the uptake, the total counts in the region of interest drawn around

[3]Authors are grateful to Prof. Howard Gendelman for allowing the use of his A-Spect scintillation camera.

the perimeter of the tumor were measured and divided by the number of pixels for each tumor at each time point and the tumor-specific uptake was obtained after subtraction of the background counts.

Statistical analyses.

Statistical analyses for in vitro studies were performed using the two-sided, unpaired Student's t-test at the significance level of ≤ 0.05. Error bars in figures represent standard error of the mean (SEM). Kaplan-Meier survival analyses were done using MedCalc Software Ver. 7.4.4.0 (Mariakerke, Belgium). To assess differences in tumor growth between treatment groups the generalized estimating equations were used[4]. The logrank test for trend analyses of tumor growth in the irradiated mice was done using the GraphPad InStat version 3.00 for Windows 95, (GraphPad Software, San Diego California).

Results and Discussion

LS174T cells do not express PDGF receptors *in vitro*, as judged by ^{125}I-PDGF-BB binding assays or by immunoblotting with anti-phosphotyrosine antibodies after stimulation with PDGF-BB (Fig. 1A). LS174T cells grown in vitro as a monolayer are effectively unresponsive to STI571. Fig. 1B shows the surviving fraction of LS174T at pharmacological threshold levels of STI571, i.e., up to 5 μM after 24 h and 48 h of exposure to STI571. Based on these in vitro data, the cytotoxicity of STI571 in xenografted tumors was not anticipated. Next, the possibility that STI571 can influence radiosensitivity was taken into consideration. To experimentally eliminate/confirm this possibility LS174T cells were grown as a monolayer and irradiated at a rate of 1.95 Gy/min, for a total radiation dose of 1 Gy or 6 Gy, in the absence or presence of different concentrations of STI571 (Fig. 1C). LS174T cells did not exhibit any particularly unusual sensitivity to radiation in the presence of STI571. Treatment with STI571 in vitro neither enhances nor inhibits radiation-induced cell death in LS174T, i.e., the external beam irradiation of in vitro grown cells in the presence of various concentrations of STI571 had only additive effects. As expected, the 6 Gy dose produced about 45% cell kill, whereas a sublethal dose of 1 Gy retarded the cell growth by 2% – 5%. The effect of combined treatment with ^{131}I-labeled antibodies and STI571 in vitro was also tested. Two monoclonal antibodies ^{131}I-anti-CEA (LS174T express CEA) and ^{131}I-B72.3 were used. Responses of in vitro grown LS174T cells to ^{131}I-labeled antibodies were not influenced by STI571.

LS174T cells grown as SQ xenografts in athymic mice develop tumors rich in connective tissue (Fig. 1D left panel). The presence of PDGFr-β in de-paraffinized, formalin-fixed 5-μsections of LS174T tumors was confirmed using polyclonal rabbit antibody 958 directed against PDGFr-β. Nonspecific rabbit IgG was used as a control (Fig. 1D right panel). Goat anti-rabbit MAb conjugated to biotin were used to amplify the signal, which was subsequently developed using a 3,3′-diaminobenzidine staining kit. PDGFr-β was detected only in tumor stroma.

The premise of the STI571-RIT approach rests on the STI571-induced changes in tumor P_{IF}. The effect of STI571 on P_{IF} in SQ LS174T xenografts was therefore measured using the wick-in-needle technique. Mice carrying LS174T tumors were divided into tumor size matched groups and either treated with vehicle or with oral (PO) doses of 50 mg/kg BID STI571, for four consecutive days. The mean tumor P_{IF} in the vehicle-treated group (n=6) was found to be 5.3 ± 0.4 mm Hg, whereas the mean tumor P_{IF} of the STI571-treated group (n=5) was significantly reduced by 55% to 2.4 ± 0.9 mm Hg (Fig. 2A; $P < 0.001$). The >45% attenuation of P_{IF}, through the STI571 inhibition of PDGFr-β in these tumors, corroborates the use of this

[4]This data analysis was done by Dr. James R. Anderson, Professor and Chairman of the Department of Preventive and Societal Medicine at UNMC

tumor model to measure the impact of STI571 on radioimmunotherapy in solid tumors. Further evidence on the involvement of STI571 in PDGFr-β - mediated improvement of radioimmunotherapy came from ELISA and blotting studies of lysates prepared from STI571-treated tumors as compared to PBS-treated tumors. The ELISA results indicate approximately 40% reduction in levels of phospho-PDGFr-β (Fig. 2B). The protein band analyses done after the Western blotting indicate that the average phosphorylation per PDGFr-β is reduced by at least 35% (data not shown). The results from both methods are virtually identical within the experimental error.

The tumor uptake and biodistribution of radiolabeled B72.3 MAb was measured in LS174T tumor-bearing mice after either PBS or STI571 administration (Table 2). The duration of the STI571 effect was also evaluated. The most effective scheme proved to be the fractionated dosing of STI571 over a period of seven to ten days, with two oral doses daily. The treatment with eight 50 mg/kg BID doses of STI571 yielded >2.4 times greater uptake of ^{125}I-B72.3 in LS174T xenografts (Table 2), compared to LS174T xenografts in mice treated with PBS (*P < 0.0001*).

The therapeutic consequences of STI571-mediated increase in tumor B72.3 MAb uptake were subsequently investigated (Fig. 2C). LS174T tumors were implanted SQ and allowed to grow for 10 days. Mice were randomized into four groups: (1) no treatment (n = 10); (2) ^{131}I-B72.3 only (n = 10); (3) STI571 only (n = 12); and (4) ^{131}I-B72.3 plus STI571 (n = 12). Body weight and tumor sizes were measured three times a week, and tumor volumes calculated. Data is plotted as a relative tumor growth normalized to the tumor size on day -3 when the first dose of STI571 was given (Fig. 2C). On the day of ^{131}I-B72.3 administration (day 0), the average tumor size in all groups was 270 ± 70 mm^3. The STI571 seven-day dosing scheme was used as shown in Table 1. In as little as one week after the 0.25-mCi (9.25 MBq) dose of ^{131}I-B72.3, the advantage of the combined treatment was apparent. Tumor sizes in mice treated with a combination STI571+RIT were less that 50% of the untreated tumors (*P = 0.009*). During this same time, radioimmunotherapy alone produced approximately a 10% decrease in tumor volume, while STI571 alone had no measurable effect. The generalized estimating equations were used to assess differences in tumor growth between treatment groups. The change in quadrupling time (Tq) was calculated on day 10 for the PBS and STI571 alone controls (termination date due to the excessive tumor burden >2,500 mm^3) and on day 28 after ^{131}I-B72.3 administration for the rest of mice (details are in Table 3). Supplementation of ^{131}I-B72.3 radioimmunotherapy with STI571 improved overall anti-tumor effects by about 220%, compared to radioimmunotherapy alone (*P = 0.008*) and confirmed that the inhibition of PDGFr-β signaling in tumor stroma and subsequent reduction in tumor P_{IF} enhances the therapeutic effects of radioimmunotherapy in solid tumors.

In vitro studies did not indicate any effects of STI571 on intrinsic radiosensitivity of LS174T tumor cells (Fig. 1C). To explore if STI571 interactions with tumor stroma altered radiosensitivity of in vivo grown tumors and thereby contributed to the therapeutic synergy, the effects of STI571 treatment on sensitivity to external beam radiation was analyzed. LS174T cells were implanted SQ, 5 × 10^6 cells/mouse, and allowed to develop tumors > 400 mm^3 (average tumor volume = 710 ± 330 mm^3). Treated mice received total of six PO doses of STI571 at 50 mg/kg body weight/dose for three days before irradiation. Control mice were given sham PO doses of PBS. Twenty-four hours after the last dose of STI571, mice were placed in a lead rig that shields the whole body and allows irradiation of tumors only. The external beam irradiations were carried out at a rate of 1.95 Gy/min for the total of 6 Gy. Mice were censored for Kaplan-Meier analyses when the tumor size tripled or exceeded 2,500 mm^3. Fig. 2D shows the summary of these results. There are no differences in the tumor growth in untreated control mice (n=8) and STI571-treated control mice (n=8) (*P=0.3297*). However, there is a difference between tumor responses in irradiated control mice (n=8) as compared to

mice treated with STI571 and radiation (n = 9; *P = 0.0553*). Moreover, the logrank test for trend indicates a statistically significant delay in tumor growth with *P = 0.0075* (*P* values were obtained in the Mantel-Haenszel logrank test by the GraphPad Software). Median survival times to tripling of tumor size were 6.5 d, 7 d, 8 d, and not determined, i.e., not reached, for untreated controls, STI571 controls, irradiated controls, and STI571+irradiation, respectively. This increase of the median survival of the STI571+external beam-treated mice, along with the logrank trend analyses, hinted that additional factors such as improved tumor perfusion and the ensuing improvements in tumor oxygenation may have also contributed to the therapeutic synergy between STI571 and RIT. Indeed, the enhanced ^{131}I-B72.3 uptake into the STI571-treated tumors proved to be only one of the factors responsible for improvements in tumor responses to radioimmunotherapy when combined with the STI571 treatment. Two additional causes both related to the STI571-induced attenuation of P_{IF}, were identified: (*1*) improved homogeneity of MAb distribution in tumor; and (*2*) increased tumor radiosensitivity in response to improved tumor oxygenation. These aspects were further characterized by analyzing in more detail the radioimmunoconjugate distribution within tumors and by analyzing tumor hypoxia.

The spatial and temporal distribution of radioimmunoconjugates in tumors after STI571 treatment was analyzed in imaging studies. Mice with size-matched tumors (1.9 – 2.1 g) were selected from groups treated for 10 days with either STI571 (n = 2) or PBS (n = 2; control), as shown in Table 1. ^{125}I-B72.3 was injected intravenously (IV) and the imaging commenced 24 h after the administration of the radioactive tracer. The greatly improved homogeneity of ^{125}I-B72.3 in STI571-treated mice is apparent in images shown in Fig. 2E. Temporal images of the STI571-treated mouse are shown in Fig. 3. On average 8,400 counts/pixel were observed in tumors of the STI571-treated mice compared to 3,700 counts/pixel in the PBS-treated mice 48 h after injection. This amounts to >220% greater uptake of the radioimmunoconjugate in the STI571-treated tumors. At 72 h postinjection these differences are even more pronounced with an average of 7,100 counts/pixel and 2,100 counts/pixel observed in STI571- and PBS-treated tumors, respectively. Noticeable gains in the retention of radioactivity are also evident in STI571-treated tumors compared to PBS controls, i.e, the efflux of radioactivity from tumors in PBS-treated mice amounts to approximately 40%/day while less than 15%/day is lost from the tumors of STI571-treated mice. This translates into a significant increase in radiation doses deposited during 24 h, from 2.6 Gy/MBq in PBS controls to 10.2 Gy/MBq in STI571-treated mice for a 2-g tumor.

It is unquestionable that the retention of ^{125}I-B72.3 and the homogeneity of its distribution in tumors treated with STI571 are significantly improved compared to PBS-treated control mice. The remarkable contrast between the homogeneity of tumor uptake in the STI571-compared to PBS-treated tumors is best apparent in the sagittal images shown in Fig. 4A. The quantitative evaluation of counts in a 6 pixels by 6 pixels regions of interest, located in the core of each tumor, confirms the gross evaluation of the images (Fig. 4B). At 72 h after administration, the enhancement of the radioimmunotherapy uptake in the STI571-treated tumors is >300%.

Effects of STI571 on tumor hypoxia were measured using a nitroimidazole-based radioiodinated hypoxia tracer, 1-[ethyl-(3′-[^{125}I]iodobenzamide)]-2-nitroimidazole (38). Mice bearing large LS174T tumors (n = 9; average tumor size 0.8 g; range 0.4 – 1.4 g) were treated with 2, 4, and 6 PO doses of STI571. Control mice received 6 PO doses of the vehicle (PBS). Forty-eight hours after the last dose of STI571, an IV dose of 0.01 mCi/mouse (0.37 MBq/mouse) 1-[ethyl-(3′-[^{125}I]iodobenzamide)]-2-nitroimidazole was given. Mice were killed 2.5 h later. Necropsy was performed and the radioactive content of several tissues, blood, and tumors was determined. The evaluation of these data is complicated by the enhanced extravasation of the tracer in response to the STI571 treatment. An approximately 35% increase in the uptake of the hypoxia marker was observed after only two doses of STI571, compared

to control mice treated with PBS. This rise in uptake is most certainly in response to the decreasing tumor P_{IF} (22,24). However, as the number of STI571 doses increased, the amount of the hypoxia marker uptake in the tumor decreased (Fig. 4C), indicating increased tumor oxygenation. It can be concluded with a reasonable certainty that this reduction of hypoxia in response to treatment with STI571 has a profoundly positive effect on the tumor responses to RIT.

In conclusion, STI571, an inhibitor of the PDGF receptor tyrosine kinase, improves the anti-cancer effects of radioimmunotherapy with ^{131}I-B72.3 antibodies in solid tumors. STI571 alone does not influence the growth of LS174T tumors. The improved responses to combination radioimmunotherapy and STI571 are the result of lowered tumor's P_{IF} brought about by the inhibition of PDGFr-β localized in the tumor stroma. The ensuing increased uptake of radioimmunotherapy into the tumor provides radiation dose deposits on the order of 400% greater in the STI571+RIT mice than in PBS-treated mice. The synergy between STI571 and radioimmunotherapy is further aided by the improved homogeneity of radioimmunotherapy distribution in tumors, and by significantly reduced tumor hypoxic fraction. This latter effect produces indirect radiosensitization of the tumor cells.

Although it cannot formally be excluded that inhibition of c-kit or abl participate in these effects, the existing biological understanding suggests that inhibition of PDGFr-β is the prime molecular mechanism for the observed effects of STI571. It should also be noted that anti-angiogenic effects of PDGF inhibitors, through targeting of PDGF receptors on endothelial cells or pericytes, have been described (39–42). To what extent these effects contribute to the antibody uptake and hypoxia, and to the therapeutic synergy, merits further studies. Findings presented here should encourage further experimental and clinical studies on the effects of STI571 on radioimmunotherapy and other radiation-based therapies.

References

1. Vose JM, Wahl RL, Saleh M, et al. Multicenter phase II study of iodine-131 tositumomab for chemotherapy-relapsed/refractory low-grade and transformed low-grade B-cell non-Hodgkin's lymphomas. J Clin Oncol 2000;18:1316–23. [PubMed: 10715303]
2. Kaminski MS, Zelenetz AD, Press OW, et al. Pivotal study of iodine I 131 tositumomab for chemotherapy-refractory low-grade or transformed low-grade B-cell non-Hodgkin's lymphomas. J Clin Oncol 2001;19:3918–28. [PubMed: 11579112]
3. Witzig TE, White CA, Gordon LI, Wiseman GA, Emmanouilides C, Murray JL, Lister J, Multani PS. Safety of yttrium-90 ibritumomab tiuxetan radioimmunotherapy for relapsed low-grade, follicular, or transformed non-hodgkin's lymphoma. J Clin Oncol 2003;21:1263–70. [PubMed: 12663713]
4. Behr TM, Goldenberg DM, Becker WS. Radioimmunotherapy of solid tumors: a review "of mice and men". Hybridoma 1997;16:101–7. [PubMed: 9085136]
5. Tempero M, Leichner P, Baranowska-Kortylewicz J, et al. High-dose therapy with 90Yttrium-labeled monoclonal antibody CC49: a phase I trial. Clin Cancer Res 2000;6:3095–102. [PubMed: 10955789]
6. DeNardo SJ, Williams LE, Leigh BR, Wahl RL. Choosing an optimal radioimmunotherapy dose for clinical response. Cancer 2002;94(4 Suppl):1275–86. [PubMed: 11877757]
7. Fand I, Sharkey RM, Grundy JP, Goldenberg DM. Localization by whole-body autoradiography of intact and fragmented radiolabeled antibodies in a metastatic human colonic cancer model. Int J Rad Appl Instrum B 1992;19:87–99. [PubMed: 1577618]
8. Blumenthal RD, Sharkey RM, Kashi R, Natale AM, Goldenberg DM. Physiological factors influencing radioantibody uptake: a study of four human colonic carcinomas. Int J Cancer 1992;51:935–41. [PubMed: 1322378]
9. DeNardo SJ, Mirick GR, Kroger LA, O'Grady LF, et al. The biologic window for chimeric L6 radioimmunotherapy. Cancer 1994;73(3 Suppl):1023–32. [PubMed: 8306244]
10. Netti PA, Hamberg LM, Babich JW, et al. Enhancement of fluid filtration across tumor vessels: implication for delivery of macromolecules. Proc Natl Acad Sci US A 1999;96:3137–42.

11. Buchsbaum DJ. Experimental approaches to increase radiolabeled antibody localization in tumors. Cancer Res 1995;55(23 Suppl):5729s–5732s. [PubMed: 7493336]
12. Postema EJ, Borjesson PK, Buijs WC, et al. Dosimetric analysis of radioimmunotherapy with 186Re-labeled bivatuzumab in patients with head and neck cancer. J Nucl Med 2003;44:1690–9. [PubMed: 14530488]
13. van Zanten-Przybysz I, Molthoff CF, Roos JC, et al. Radioimmunotherapy with intravenously administered 131I-labeled chimeric monoclonal antibody MOv18 in patients with ovarian cancer. J Nucl Med 2000;41:1168–76. [PubMed: 10914906]
14. Kurizaki T, Okazaki S, Sanderson SD, et al. Potentiation of radioimmunotherapy with response-selective peptide agonist of human C5a. J Nucl Med 2002;43:957–67. [PubMed: 12097469]
15. Hornick JL, Sharifi J, Khawli LA, et al. A new chemically modified chimeric TNT-3 monoclonal antibody directed against DNA for the radioimmunotherapy of solid tumors. Cancer Biother Radiopharm 1998;13:255–68. [PubMed: 10850361]
16. DeNardo GL, O'Donnell RT, Kroger LA, et al. Strategies for developing effective radioimmunotherapy for solid tumors. Clin Cancer Res 1999;5(10 Suppl):3219s–3223s. [PubMed: 10541367]
17. Akabani G, Reist CJ, Cokgor I, et al. Dosimetry of 131I-labeled 81C6 monoclonal antibody administered into surgically created resection cavities in patients with malignant brain tumors. J Nucl Med 1999;40:631–8. [PubMed: 10210222]
18. Sharkey RM, McBride WJ, Karacay H, et al. A universal pretargeting system for cancer detection and therapy using bispecific antibody. Cancer Res 2003;63:354–63. [PubMed: 12543788]
19. de Lange Davies C, Engesaeter BO, Haug I, Ormberg IW, Halgunset J, Brekken C. Uptake of IgG in osteosarcoma correlates inversely with interstitial fluid pressure, but not with interstitial constituents. Br J Cancer 2001;85:1968–77. [PubMed: 11747342]
20. Pluen A, Boucher Y, Ramanujan S, et al. Role of tumor-host interactions in interstitial diffusion of macromolecules: cranial vs. subcutaneous tumors. Proc Natl Acad Sci USA 2001;98:4628–33. [PubMed: 11274375]
21. el-Kareh AW, Secomb TW. Effect of increasing vascular hydraulic conductivity on delivery of macromolecular drugs to tumor cells. Int J Radiat Oncol Biol Phys 1995;32:1419–23. [PubMed: 7635782]
22. Pietras K, Ostman A, Sjoquist M, et al. Inhibition of platelet-derived growth factor receptors reduces interstitial hypertension and increases transcapillary transport in tumors. Cancer Res 2001;61:2929–34. [PubMed: 11306470]
23. Pietras K, Rubin K, Sjoblom T, et al. Inhibition of PDGF receptor signaling in tumor stroma enhances antitumor effect of chemotherapy. Cancer Res 2002;62:5476–84. [PubMed: 12359756]
24. Pietras K, Stumm M, Hubert M, Buchdunger E, et al. STI571 enhances the therapeutic index of epothilone B by a tumor-selective increase of drug uptake. Clin Cancer Res 2003;9(10 Pt 1):3779–87. [PubMed: 14506171]
25. Rodt SA, Ahlen K, Berg A, Rubin K, Reed RK. A novel physiological function for platelet-derived growth factor-BB in rat dermis. J Physiol 1996;495(Pt 1):193–200. [PubMed: 8866362]
26. Heuchel R, Berg A, Tallquist M, et al. Platelet-derived growth factor beta receptor regulates interstitial fluid homeostasis through phosphatidylinositol-3′ kinase signaling. Proc Natl Acad Sci USA 1999;96:11410–5. [PubMed: 10500190]
27. Capdeville R, Silberman S. Imatinib: a targeted clinical drug development. Semin Hematol 2003;40 (2 Suppl 2):15–20. [PubMed: 12783370]
28. Ebnoether M, Stentoft J, Ford J, Buhl L, Gratwohl A. Cerebral oedema as a possible complication of treatment with imatinib. Lancet 2002;359:1751–2. [PubMed: 12049868]
29. Shimazaki C, Ochiai N, Uchida R, et al. Intramuscular edema as a complication of treatment with imatinib. Leukemia 2003;17:804–5. [PubMed: 12682642]
30. Tom BH, Rutzky LP, Jakstys MM, Oyasu R, Kaye CI, Kahan BD. Human colonic adenocarcinoma cells. I. Establishment and description of a new line In Vitro 1976;12:180–91.
31. Johnson VG, Schlom J, Paterson AJ, Bennett J, Magnani JL, Colcher D. Analysis of a human tumor-associated glycoprotein (TAG-72) identified by monoclonal antibody B72. 3 Cancer Res 1986;46:850–7. [PubMed: 3940648]

32. Schlom J, Eggensperger D, Colcher D, et al. Therapeutic advantage of high-affinity anticarcinoma radioimmunoconjugates. Cancer Res 1992;52:1067–72. [PubMed: 1310638]
33. Alvarez RD, Huh WK, Khazaeli MB, et al. A Phase I study of combined modality (90)Yttrium-CC49 intraperitoneal radioimmunotherapy for ovarian cancer. Clin Cancer Res 2002;8:2806–11. [PubMed: 12231520]
34. Fraker PJ, Speck JC Jr. Protein and cell membrane iodinations with a sparingly soluble chloroamide, 1,3,4,6-tetrachloro-3a,6a-diphrenylglycoluril. Biochem Biophys Res Commun 1978;80:849–57. [PubMed: 637870]
35. Uhrbom L, Hesselager G, Östman A, Nistér M, Westermark B. Dependence of autocrine growth factor stimulation in platelet-derived growth factor-B-induced mouse brain tumor cells. Int J Cancer 2000;85:398–406. [PubMed: 10652433]
36. Eriksson A, Siegbahn A, Westermark B, Heldin CH, Claesson-Welsh L. PDGF alpha- and beta-receptors activate unique and common signal transduction pathways. EMBO J 1992;11:543–550. [PubMed: 1311251]
37. Claesson-Welsh L, Hammacher A, Westermark B, Heldin CH, Nister M. Identification and structural analysis of the A type receptor for platelet-derived growth factor. Similarities with the B type receptor. J Biol Chem 1989;264:1742–1747. [PubMed: 2536372]
38. Cherif A, Wallace S, Yang DJ, et al. Development of new markers for hypoxic cells: [131I] Iodomisonidazole and [131I]Iodoerythronitroimidazole. J Drug Target 1996;4:31–9. [PubMed: 8798876]
39. Buchdunger E, O'Reilly T, Wood J. Pharmacology of imatinib (STI571). Eur J Cancer 2002;385:S28–36. [PubMed: 12528770]
40. Uehara H, Kim SJ, Karashima T, et al. Effects of blocking platelet-derived growth factor-receptor signaling in a mouse model of experimental prostate cancer bone metastases. J Natl Cancer Inst 2003;95:458–70. [PubMed: 12644539]
41. Apte SM, Fan D, Killion JJ, Fidler IJ. Targeting the platelet-derived growth factor receptor in antivascular therapy for human ovarian carcinoma. Clin Cancer Res 2004;10:897–908. [PubMed: 14871965]
42. Erber R, Thurnher A, Katsen AD, et al. Combined inhibition of VEGF and PDGF signaling enforces tumor vessel regression by interfering with pericyte-mediated endothelial cell survival mechanisms. FASEB J 2004;18:338–40. [PubMed: 14657001]

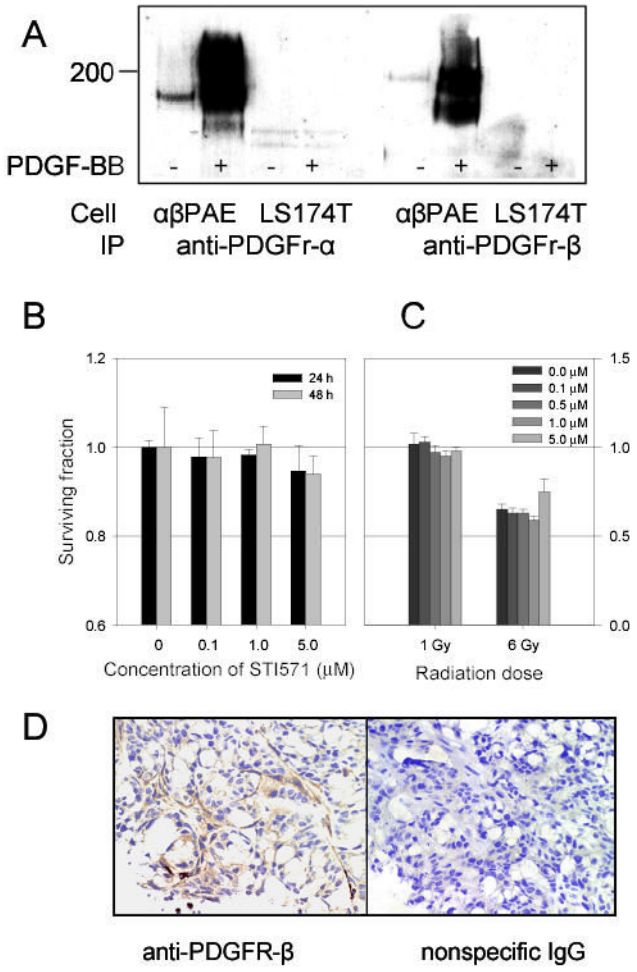

Figure 1.

Characterization of PDGFr-β interactions with STI571 in LS174T cells in vitro and in vivo. **A**. Immunoblot of human adenocarcinoma LS174T cells and porcine aortic endothelial cells expressing the PDGFr-α and -β (αβ -PAE) (control). Cells were left untreated or were stimulated with PDGF-BB and following sequential immunoprecipitation (IP) of PDGF receptors, immunoblotting to detect activated PDGFr was performed using anti-phosphotyrosine antibodies. **B**. Survival of LS174T cells in the presence of low concentrations of STI571. Cells were treated for 24 h or 48 h with STI571 and subsequently the metabolic/proliferative activities measured. The surviving fraction of the untreated control cells is one. **C**. Survival of LS174T cells grown in the presence of various STI571 concentrations and irradiated with 1 Gy and 6 Gy. **D**. Immunohistochemical staining using antibodies against PDGFr-β or nonspecific rabbit IgG as a control in 5-μ sections of formalin-fixed LS174T tumors.

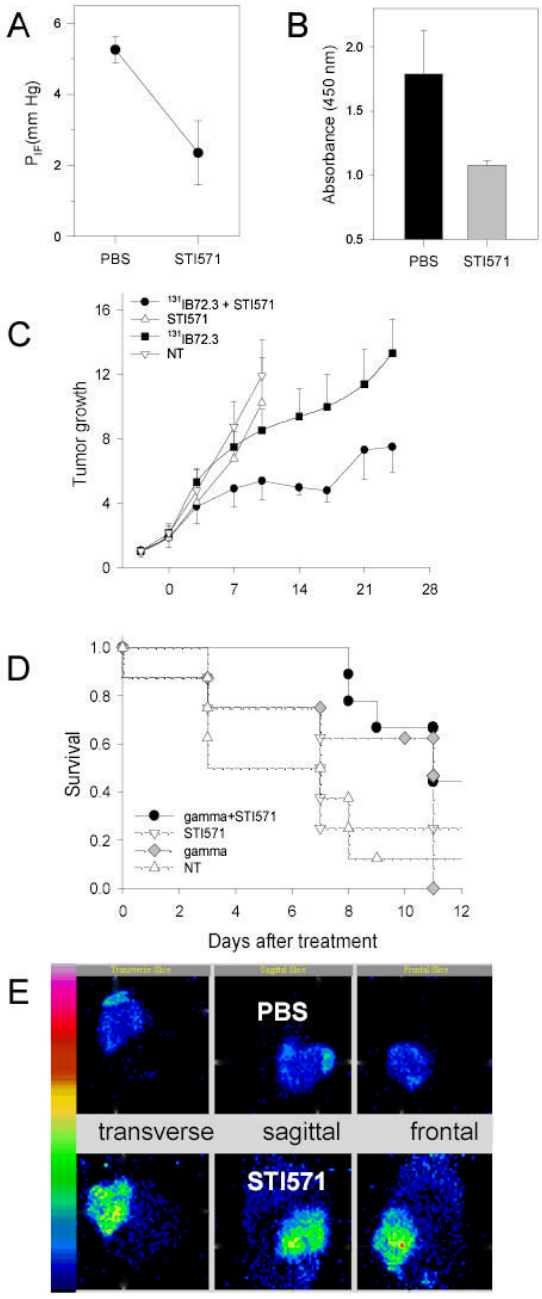

Figure 2.

Response of LS174T tumors to various treatments with STI571. **A**. Changes in the tumor interstitial fluid pressure P_{IF}. Tumor-bearing mice received vehicle (n=6) or STI571 (n=5) for four consecutive days before the measurement of tumor P_{IF}. **B**. Impact of STI571 on the production of phospho-PDGFr-β in LS174T tumors grown as SQ xenografts in athymic mice treated with either PBS (control) or STI571 (n = 15 to 18). **C**. Arrest of LS174T tumor growth in response to the combination radioimmunotherapy and STI571 treatment. Mice were treated as outlined in Table 1. Data is plotted as a relative tumor growth normalized to the tumor size on day -3 when the first dose of STI571 was given. **D**. Kaplan-Meier analysis of the response of LS174T xenografts to the external beam radiotherapy in mice treated with PO doses of either

PBS or STI571. **E**. Single photon emission computed tomography images (SPECT) acquired 72 h after administration of ^{125}I-B72.3 in LS174T-bearing mice treated with PBS (control) or STI571 as shown in Table 1. The PBS-treated tumor had an early onset of ulceration typical of LS174T tumors of this size. The pooling of the blood in the area of the ulcer is clearly noticeable in images shown in Fig.2E and in panels 16, 19, and 22 of Fig. 4A (NT).

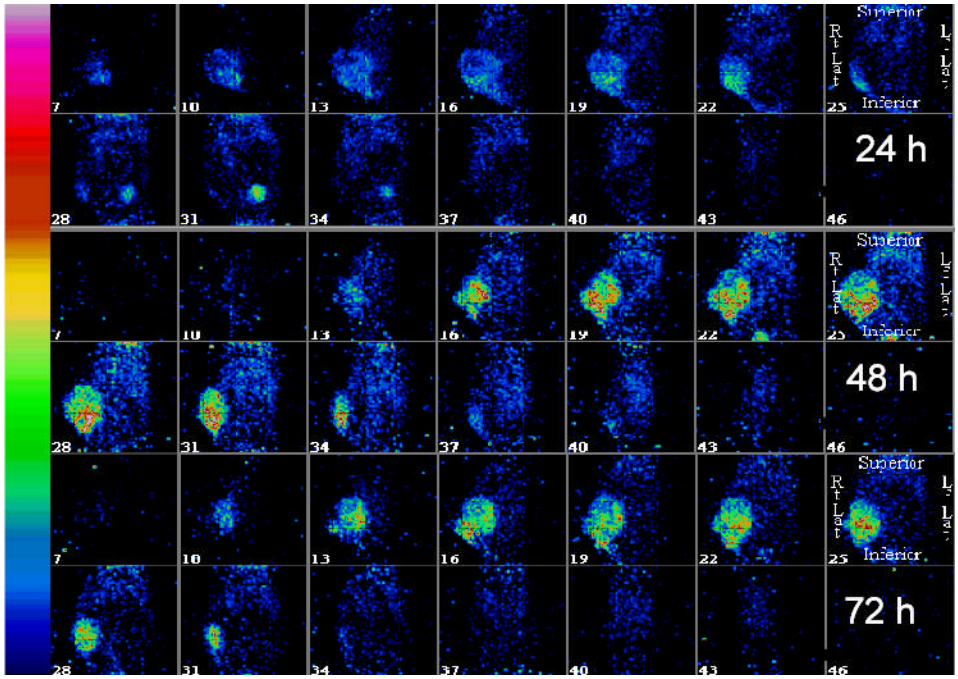

Figure 3.
SPECT images of athymic mice bearing SQ LS174T xenografts acquired with the LumaGEM™ scintillation camera. Mice treated with STI571 as indicated in Table 1 and their images acquired 24, 48, and 72 h after the administration of ^{125}I-B72.3.

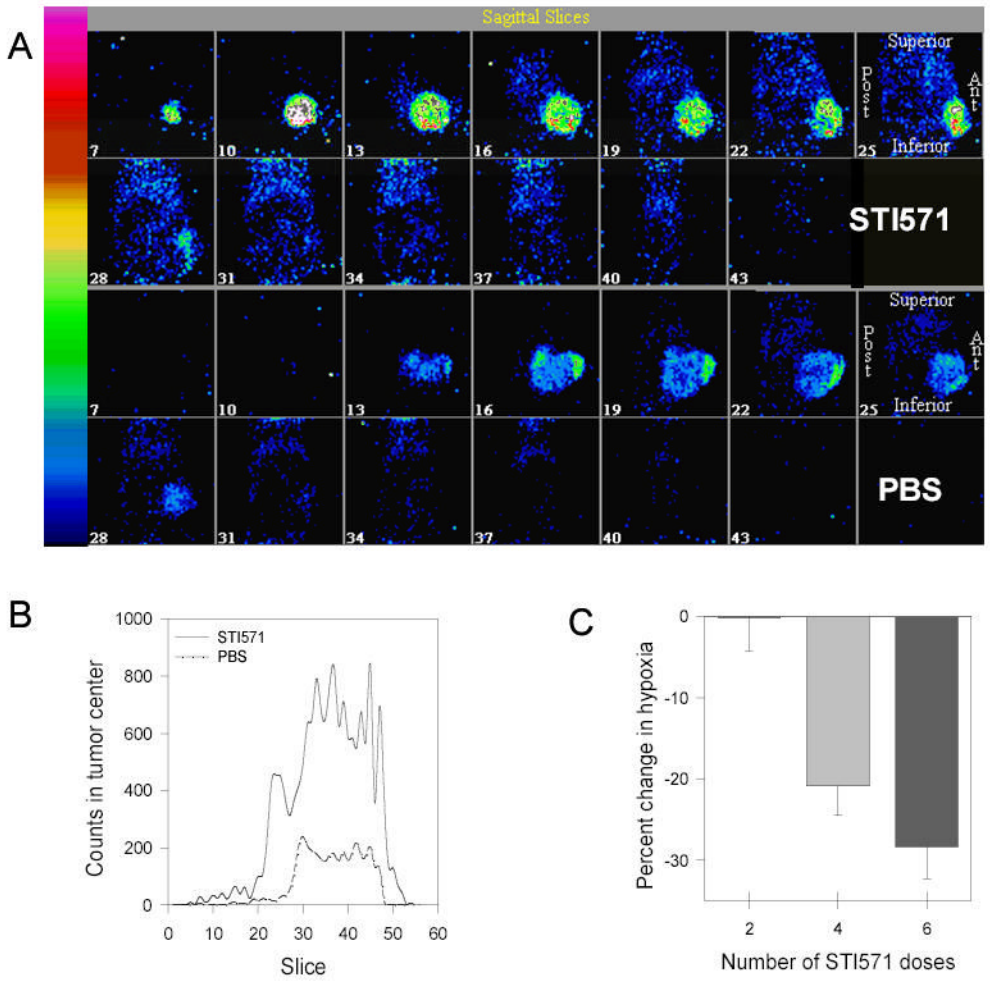

Figure 4.

The effect of STI571 on the tumor uptake of the radioactive tracers. **A**. Comparison of ^{125}I-B72.3 uptake in tumors of STI571- treated (upper panels) and PBS-treated (lower panels) mice 72 h after the administration of radioactivity. Images were acquired using a radius of rotation of 3.29 cm and a pixel size of 0.78 mm. Volume images have been reconstructed and the Butterworth bandpass postfiltering was applied. **B**. Differences in the tumor uptake of ^{125}I-B72.3 in the center of the tumor. The size of the region of interest was 6 × 6 pixels size (4.68 mm × 4.68 mm) and was located in the core of the tumor; the diameter of tumor was 8.7 mm (PBS) and 8.9 mm (STI). **C**. Changes in the tumor hypoxia in response to STI571 treatment as determined by the tumor uptake of 1-[ethyl-(3′-[^{125}I]iodobenzamide)]-2-nitroimidazole. Data are expressed as the decrease in tumor-associated radioactivity relative to the radiotracer uptake after two doses of STI571.

Table 1

Dosing schedules for biodistribution and radioimmunotherapy studies.

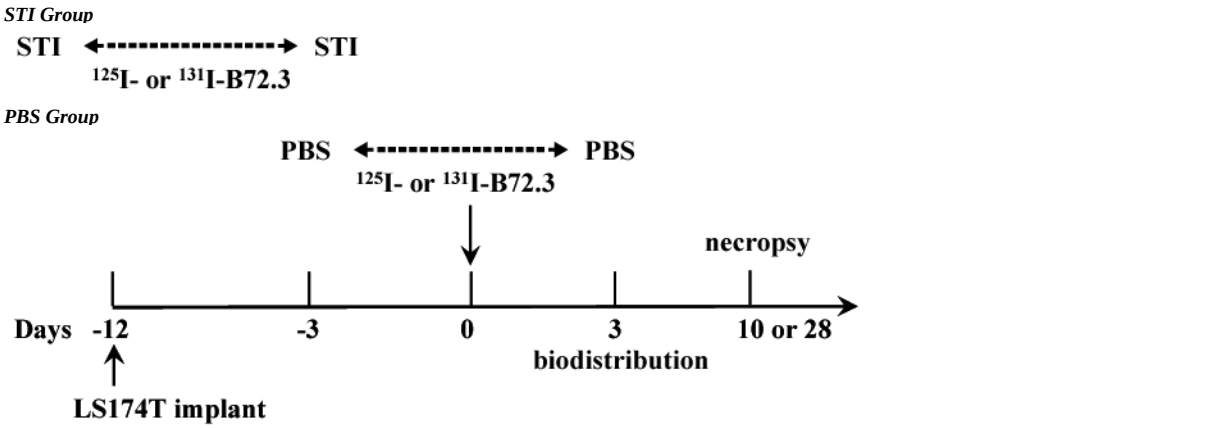

Table 2

Biodistribution of ^{125}I-B72.3 in LS174T-bearing mice treated with STI571 or PBS according to the schedule shown in Table 1.

	PBS 120 hr (n=8) average (std error)	STI571 120 hr (n=11) average (std error)
blood	1.38 (0.42)	4.45 (0.34)
liver	0.79 (0.26)	1.58 (0.14)
spleen	0.70 (0.19)	1.20 (0.11)
heart	0.29 (0.08)	0.93 (0.08)
lungs	0.66 (0.22)	2.03 (0.16)
kidneys	0.46 (0.09)	0.91 (0.08)
intestine	0.15 (0.04)	0.48 (0.04)
muscle	0.17 (0.08)	0.38 (0.04)
bone	0.19 (0.06)	0.58 (0.06)
skin	0.42 (0.14)	1.23 (0.12)
tumor	9.43 (2.53)	23.18 (2.48)

Table 3

Effect of radioimmunotherapy and combination RIT+STI571 on doubling times of LS174T xenografts in athymic mice.

	Td(days) avg (std)	Tumor growth delay
no treatment (n =6)	7.74 (1.34)*	1
STI571 (n = 10)	7.75 (1.20)*	1
^{131}I-B72.3 (n = 6)	18.95 (2.98)**	2.4
STI571 plus 131I-B72.3 (n = 9)	40.63 (8.43)**	5.2

* day 10;

** day 28;